

Thickness effect on the dielectric, ferroelectric, and piezoelectric properties of ferroelectric lead zirconate titanate thin films

J. Pérez de la Cruz,^{1,a)} E. Joanni,¹ P. M. Vilarinho,² and A. L. Kholkin²

¹*Optoelectronics and Electronic Systems Unit, INESC-Porto, Rua do Campo Alegre 687, 4169-007 Porto, Portugal*

²*Department of Ceramic and Glass Engineering, CICECO, University of Aveiro, 3810-193 Aveiro, Portugal*

(Received 29 September 2010; accepted 15 October 2010; published online 6 December 2010)

Lead zirconate titanate ($\text{PbZr}_{0.52}\text{Ti}_{0.48}\text{O}_3$ -PZT) thin films with different thicknesses were deposited on Pt(111)/Ti/SiO₂/Si substrates by a sol-gel method. Single perovskite phase with (111)-texture was obtained in the thinnest films, whereas with the increase in thickness the films changed to a highly (100)-oriented state. An increase in the mean grain size as the film thickness increased was also observed. Dielectric, ferroelectric, and piezoelectric properties were analyzed as a function of the film thickness and explained based on film orientation, grain size, domain structure, domain wall motion, and nonswitching interface layers. Both serial and parallel capacitor models were used to analyze the influence of the nonswitching interface layer in the dielectric properties and the effect of substrate clamping in the microscopic piezoelectric response as the film thickness decreased. The scanning force microscopy technique was used to study the effect of thickness on the microscopic piezoresponse. Significant differences between the macroscopic and microscopic electrical properties of the films were observed. Those differences can be assigned to changes in the nonswitching film-electrode layer and domain structure. © 2010 American Institute of Physics.

[doi:10.1063/1.3514170]

I. INTRODUCTION

Thin film ferroelectric materials have been investigated for a variety of device applications such as follows: nonvolatile ferroelectric memories,¹ piezoelectric sensors and actuators,² pyroelectric detectors,³ and capacitors in dynamic random access memories (DRAM).⁴ Among the most popular ferroelectric thin film materials is the lead zirconate titanate ($\text{PbZr}_x\text{Ti}_{1-x}\text{O}_3$), especially the compositions around the morphotropic phase boundary. Its popularity is based on the potential applications in logic memory devices due to its large remanent polarization (Pr), relatively small coercive field and high dielectric constant.⁵ It is also an excellent material for piezoelectric devices due to its high d_{33} coefficient.⁶ However, all these properties are conditioned by the lead zirconate titanate (PZT) films thickness.

The present trend of electronic miniaturization requires scaling down the thickness of ferroelectric system below ~150 nm.^{7,8} Thus, an understanding of the influence of film thickness on the ferroelectric stability is considered imperative for the main ferroelectric thin film applications. Since ferroelectricity is a collective phenomenon, its occurrence is associated with a critical correlation volume, below which it should be lost.⁹ However, other factors should be taken into account in the monitoring of the ferroelectric properties; for instance, the increasing role of the electrode-film interface layer as the dimensions is reduced.¹⁰⁻¹² As such, the analysis of the thickness dependence of dielectric, ferroelectric and piezoelectric properties of the films is decisive in the development and implementation of several applications. High-resolution techniques, like scanning force microscopy

(SFM), in conjunction with conventional electrical measurements provide the opportunity to archive a unique insight into the real physical processes occurring in ferroelectric thin films.¹³⁻¹⁵

In this paper, the dielectric, ferroelectric, and piezoelectric properties of high-quality PZT films are studied as a function of film thickness. Moreover, the local electrical properties of the PZT films obtained by the SFM technique are compared with the macroscopic piezoelectric properties obtained by interferometric technique.

II. EXPERIMENTAL PROCEDURE

Thin-film $\text{PbZr}_{0.52}\text{Ti}_{0.48}\text{O}_3$ capacitors with different numbers of layers (2, 4, 6, 8, and 10) were deposited onto platinumized silicon substrates (Pt(111)/Ti/SiO₂/Si) using a modified sol-gel solution, as reported elsewhere.^{16,17} Each coating layer was dried at 200 °C for 2 min and pre-annealed at 500 °C for 10 min. When the desired number of layer was archived, it was annealed at 600 °C for 1 h.^{16,17}

X-ray diffraction patterns of the prepared films were obtained using a Rigaku D-max diffractometer equipped with copper K_α radiation. The measurements were performed in a step mode (0.01°/10 s), from 20° to 80° in two theta. Scanning electron microscopy (SEM) measurements were carried out by using a field emission Hitachi S4100 equipment, running at 25 kV@11 mA.

Dielectric and ferroelectric macroscopic measurements were performed using HP 4284A LCR meter and AIXACT TF analyzer light equipment, respectively. A double-beam laser interferometer with active stabilization of the working point and sensitivity about 3×10^{-4} Å, [better than analogous setups, Pan *et al.*, (Ref. 18) and Kholkin *et al.*, (Ref. 19)

^{a)}Electronic mail: jcruz@inescporto.pt.

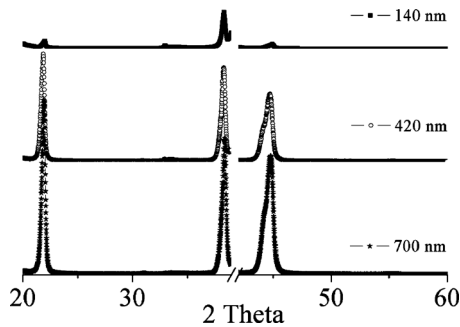


FIG. 1. X-ray diffraction patterns of PZT films with (■) 140 nm, (○) 420 nm, and (▲) 700 nm thicknesses.

due to better thermal and acoustical isolation of the active part] was used for measuring the d_{33} piezoelectric coefficient of the films. The details of the interferometric measurements are reported elsewhere.^{6,16}

Topography and domain images of the films were obtained using a scanning force microscope equipped with a Digital Instruments Nanoscope IIIa scanning probe microscope controller and a hard silicon conducting tip.²⁰ A small ac electric field of variable amplitude and 50 kHz frequency was applied between the tip and the bottom electrode in order to induce local vibration. The atomic force microscope (AFM) tip signals (amplitude and phase) were detected by a lock-in amplifier. Finally, the topography and domain images were processed using WSXMBETA6_0 software.²¹

III. RESULT AND DISCUSSION

A. Structural analysis

Figure 1 shows the x-ray diffraction patterns of PZT films with different numbers of coating layers. All the films show peaks belonging to a pure perovskite $\text{PbZr}_{0.52}\text{Ti}_{0.48}\text{O}_3$ phase. The (100), (001), (111), (200), and (002) diffraction peaks show strong thickness dependence, manifested by a clear variation in their relative intensities as the number of coating layers increases. For instance, the relative intensity of the (111) peak decreases as the number of coating layers increases. Thinnest film (two layers) shown an appreciable (111) orientation, however with the progressive increase in the thickness, the predominant orientation changes from (111) to (100)/(001).

Figure 2 shows the SEM cross-section microstructure images of PZT films with two, four, and ten coating layers. The dense microstructure with an incipient columnar grain growth is characteristic of all the prepared films. The images also allow the measurement of film thickness: ~ 140 nm (two coating layers), ~ 280 nm (four coating layers) and ~ 700 nm (ten coating layers), corresponding to a thickness of 70 nm for each deposited layer. The film thicknesses obtained by this method were used for calculate the dielectric and ferroelectric parameters. The surface microstructure (SEM plan-view) of the 140, 280, and 700 nm thick PZT films is shown in Fig. 3. Well-defined PZT grains without any rosette-type defects, typical of pyrochlore phases, are

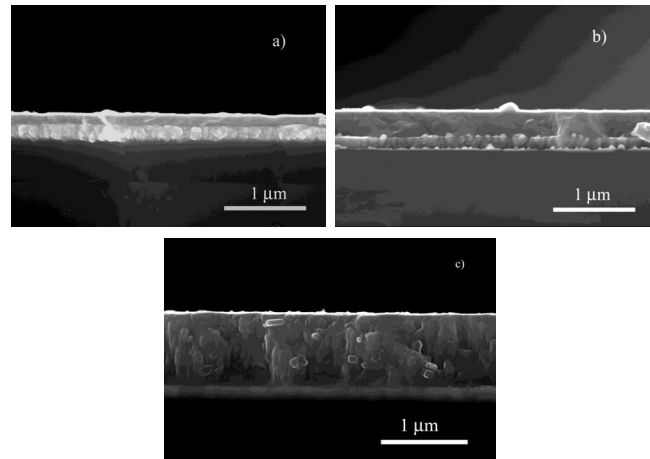


FIG. 2. SEM images of the cross-section of PZT films with (a) 2, (b) 4, and (c) 10 coating layers showing the evolution of film thickness with the number of coatings.

observed in SEM measurements. Moreover, a closed look to the three images reveals that the grain sizes change with the increase in film thickness.

Figure 4 shows the average grain sizes of PZT films as a function of film thickness. The results show that the mean grain sizes increase with increasing thickness. This result can be attributed to the higher thermal budget as the number of pyrolysis steps increases during sequential film deposition. The grain size development in thicker films is mainly controlled by the rapid grain growth due to the grain impingement resulting from the successive pyrolysis steps and the final annealing temperature. Meanwhile, in thinner films the growth is effectively linear due to the small number of pyrolysis steps, as reported by Yang *et al.*, (Ref. 22). It might be possible that this grain growth behavior somehow affects the dielectric, ferroelectric, and piezoelectric properties of the films.

B. Macroscopic dielectric properties

1. Thickness dependence of the dielectric properties

Figure 5 shows the thickness dependence of the dielectric permittivity and dielectric loss for the PZT thin films.

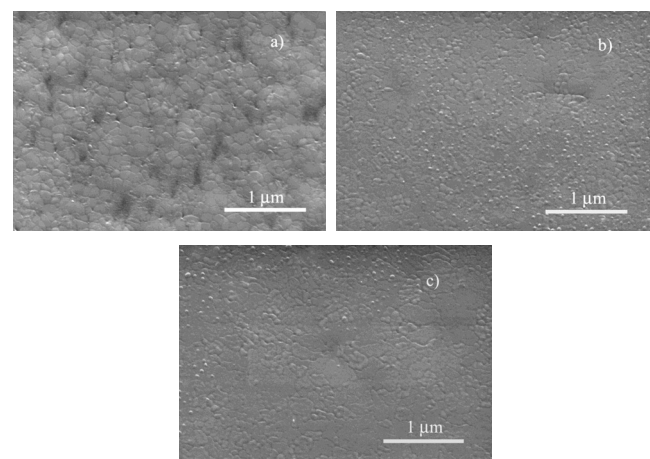


FIG. 3. SEM plan-view images of (a) 140 nm, (b) 280 nm, and (c) 700 nm thick PZT films showing the evolution of grain size with film thickness.

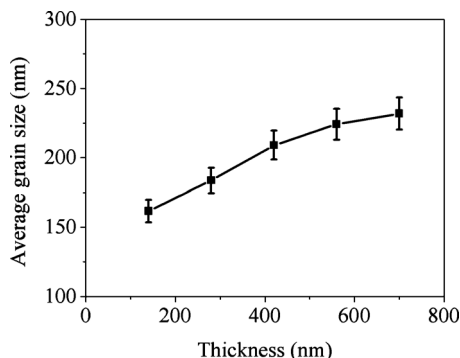


FIG. 4. Mean grain size as a function of PZT film thickness.

The dielectric permittivity (ϵ) increases continuously from 848 for the 140-nm thick PZT film up to 1270 for the 700 nm thick PZT films. Meanwhile, the dielectric loss curve shows a practically constant behavior with a relatively high loss value for all thicknesses. It is well known that the dielectric permittivity of ferroelectric films consists of two contributions: intrinsic and extrinsic,²³ which could be modified by different factors. There are a number of parameters that can affect the intrinsic contribution; among them, the more important ones are: film orientation, grain size and the mechanical stress from substrate clamping.

Preferential orientation is extremely important, since it dictates the angles between the allowable polarization vectors and the normal to the film plane. This fact could explain fairly well the contribution of the intrinsic dielectric constant to the global response measured in films with different textures. For instance, tetragonal (100)-oriented PZT films show lower relative dielectric permittivity than (111)-oriented films, as reported by Gong *et al.*, (Ref. 24). Based on this fact alone, the dielectric constant of the PZT films prepared in this work should decrease as the film thickness increases, since the orientation changes from (111) to (100) as the number of layers increase (see Fig. 1).

The second factor that must be taken into account for the intrinsic contribution is the film grain size. As the film grain size decreases, there is an increase in the internal stresses due to the difficulty in forming non-180° domains. Therefore, the intrinsic dielectric constant should increase as the grain size decreases.²⁵ This should result in a higher dielectric constant for thin films with small thicknesses, as shown in Fig. 4.

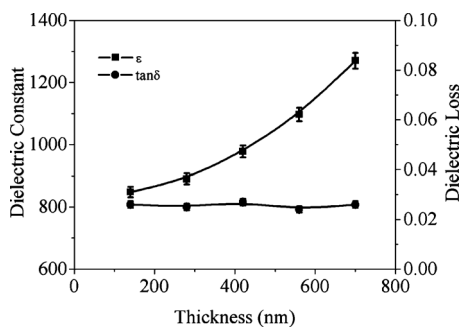


FIG. 5. Thickness dependence of the dielectric permittivity and dielectric losses of PZT films.

The third effect (mechanical stress provoked by substrate clamping) is also very important, being one of the most studied factors.^{26,27} Due to the mechanical constraints imposed by the substrate, the domain wall motion in PZT thin films is at least partially clamped and this clamping should decrease the dielectric constant. For that reason, the decrease in film thickness could be understood as an increase in the clamping effect and should bring about a subsequent decrease in the measured dielectric constant.

On the other hand, the mechanisms affecting the extrinsic contribution to the dielectric constant are not so clearly understood at present. One possibility could be associated with the hypothesis that pinning centers could appear at the interface between the bottom electrode and the ferroelectric PZT film.²⁸ In thicker films, a smaller relative volume would be affected by these interface pinning centers. Therefore, the 180° domain wall motion becomes easier as the thickness increases, as reported by Xu *et al.*, (Ref. 23). This corresponds to an increase in the dielectric constant as the film thickness increases. Another possibility is the influence of grain size on pinning. In small grains, the average grain boundary area (where the domain wall can be trapped by space charges) is larger than in big grains. As a result, the domain wall pinning is expected to be stronger in fine-grained films.²⁹ The aforesaid could be interpreted as a decrease in the dielectric constant as the film thickness decreases (see Fig. 4).

According to our results, the extrinsic contribution to the dielectric constant of ferroelectric PZT films with compositions near the morphotropic phase boundary (MPB) is mainly governed by domain wall mobility. Two types of domain walls are present in ferroelectric materials; 180° domain walls and non-180° domain walls. Since there is no strain change associated with 180° domain wall motion, it contributes only to the dielectric properties.²³ Thus, 180° domain walls can be considered purely ferroelectric walls. In contrast, non-180° domain walls have both ferroelectric and ferroelastic character; they can be excited either by electrical or mechanical stimuli.^{23,30} In this case, wall motion can cause changes in both polarization and strain, so that it can contribute to both the dielectric and piezoelectric properties. Non-180° domain wall motions in small grain (<200 nm) PZT thin films are believed to be very rare, due to monodomain formation. Therefore, the extrinsic contribution to the dielectric constant of ferroelectric PZT films can be mainly attributed to 180° domain wall motions.

As a result, it is possible to say that in thinnest films the dielectric loss is potentially affected by several factors (i.e., domain wall pinning, dc conductivity, space-charges, etc.). As the film thickness increases the dielectric loss is practically not affected by these factors or their influences are somehow compensated.

In summary, the contributions of intrinsic and extrinsic factors to the dielectric properties as the film thickness increase are apparently unpredictable, sometimes improving and sometimes deteriorating the properties, and in some cases (e.g., grain size) affecting the intrinsic and extrinsic contributions in opposite directions. However, as a general rule, if one considers that the extrinsic contributions are usu-

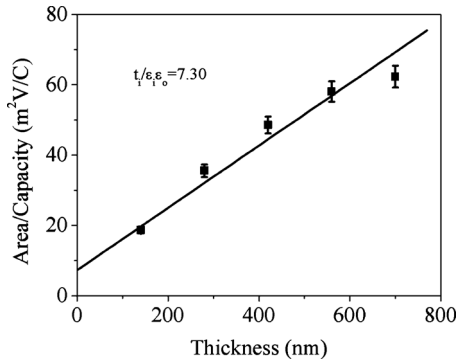


FIG. 6. Thickness dependence of the inverse capacitance density of PZT films.

ally dominant, it is expected that the dielectric properties should increase as the PZT film thickness increases, in conformity with the results shown in Fig. 5.

2. Contribution of the film-electrode interface to the dielectric properties

Besides the extrinsic contributions already discussed, another important extrinsic factor is the presence of a low-dielectric-constant layer at the film-electrode interface, which could cause a noticeable decrease in the average dielectric constant of thin films as their thickness decreases. The presence of an interfacial layer with a smaller dielectric constant can be inferred when a plot of the effective dielectric constant of PZT as a function of inverse thickness, like the one in Fig. 6, is analyzed. As discussed by Larsen *et al.*, (Ref. 10) it is expected that in homogeneous PZT films containing an interfacial layer the effective dielectric constant of the capacitor should be strongly affected in thinner films and asymptotically approach the bulk dielectric constant as the film thickness increases, as represented in Eq. (1).

The films thickness dependence observed in Fig. 5 could be easily attributed to the presence of a film-electrode layer with reduced capacitance density, C_i/A , (represented by the nonzero intercept in Fig. 6), in series with the thickness-dependent capacitance density of the film bulk.¹⁰ This constant capacitance is usually thought to represent some type of interface layer (dead layer) between the dielectric and one or both electrodes, and might arise from surface contamination of the PZT, nucleation, or reaction layers at the film-electrode interfaces, or changes in the defect chemistry.^{31,32} The apparent capacitance density at zero field may then be expressed as follows:

$$\frac{A}{C_{app}} = \frac{A}{C_i} + \frac{A}{C_B} = \frac{t}{\epsilon_{eff}} = \frac{t_i}{\epsilon_i \epsilon_o} + \frac{t - t_i}{\epsilon_B \epsilon_o}, \quad (1)$$

where A is the surface area, C_{app} is the apparent capacitance, C_i is the interface capacitance, C_B is the film bulk capacitance, ϵ_{eff} is the effective permittivity, ϵ_B is the film “bulk” permittivity, ϵ_i is the interface layer permittivity, ϵ_o is the permittivity of free space, t is the total film thickness, and t_i is the interface layer thickness.

Figure 6 shows the thickness dependence of the inverse capacitance density for PZT thin films. The straight-line intercept with the y-axis gives the ratio between the dead layer

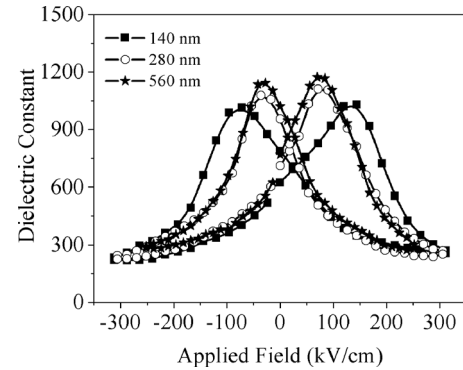


FIG. 7. Typical C - V curves of PZT thin films with different thicknesses.

thickness and its permittivity. Note that, at this point, we have no information on separate values of t_i and ϵ_i , but only on their combined effect on series capacitance. Considering the thickness of the dead layer in the range of 1–5 nm and assuming the value of the intercept ($t_i/\epsilon_i\epsilon_o=7.30$), it is possible to obtain the permittivity of the dead layer (between 15 and 75). This means that in thinner films the dielectric constant could be completely controlled by the film-electrode interlayer; meanwhile, in thicker films the dielectric constant is almost independent of this interlayer.

C. Macroscopic ferroelectric properties of PZT films as a function of thickness

1. Characteristic C - V curves of PZT films with different thicknesses

In a first approximation the capacitance-voltage (C - V) dependence may be expressed by Eq. (2) as follows:

$$C = \epsilon_{lin} \epsilon_o A / t + dP/dV, \quad (2)$$

where ϵ_{lin} is the linear dielectric constant, P is the film polarization, and V is the driving voltage. It is possible to see in this expression that the C - V behavior reveals the nonlinearity of ferroelectric thin film properties.

Figure 7 shows the C - V curves of the PZT films with different thicknesses. In all cases, the dielectric constant (capacitance) increases with increasing driving fields (driving voltage) in the low field region (It is considered that the higher electrical field can excite more reversible domain-wall motion, which contributes greatly to dielectric properties of films). After this initial electric field range, the C - V curves show a peak at the coercive field (E_c), which is due to high domain-wall density and mobility; however, as the driving field increases beyond the coercive field, the capacitance decreases abruptly. In fact, the complicated PZT domain structure tends to coalesce to a metastable state, involving not only the alignment of spontaneous polarization orientations but also the disappearance of domain walls.²⁴ Therefore, it is reasonable to assume that the baseline in the capacitances is purely associated with the intrinsic contribution.²⁴

As shown in Fig. 7, the dielectric constant increases gradually as the film thickness increases. The curves show variation in the position of the dielectric constant peaks with the thickness up to 280 nm, remaining constant for thicker films. As above mentioned, the C - V peak position corre-

sponds to the coercive field, which is affected by the decrease in thickness. The increase in the coercive field as the PZT film thickness decreases could be attributed, among other reasons, to a drastic decrease in the 180° domain wall mobility²³ and/or to the existence of dead layer at the ferroelectric-electrode interface that has a reduced dielectric constant.^{10,33} It is expected that the decrease in the films thickness results in a higher relative volume affected by the interface pinning centers and stronger domain wall pinning (small grains, Fig. 4). Both factors reduce the domain switching, increasing the driving electric field necessary to archive domain orientation.

The existence of a dead layer (*nonswitching layer*) at the ferroelectric-electrode interface could explain the increase in the coercive field as the thickness decreases. Disregarding the microscopic nature of this phenomenon, the mechanism can be described by Eq. (3) that shows the relation between the applied driving field (E) and the actual field applied to the ferroelectric (E_{eff}) as follows:^{34,35}

$$E_{\text{eff}} = E - \frac{t_i}{\epsilon_i \epsilon_o t} P. \quad (3)$$

This equation is valid in the case of practical interest where $t_i/t \ll 1$ and shows a voltage drop in the electrode-film interface. This means that the field experimented by the films is lower than the applied driving field, especially as the effective film thickness (t) decreases.

An important issue not taken into account in this analysis is the injection of electrical charges through the dead layer due to high applied electric fields. This effect should increase as the films thickness decreases [Eq. (2)]. The injection plays an important role in the switching process because any increase in the charge injection could be understood as an increase in the number of interface pinning centers and/or domain wall pinning centers.^{11,36} The hypothesis of the dead interfacial layer clearly explains the increase in the coercive field as the film thickness decreases, either by the drop of the effective electric field or by the increase in the number of pinning centers.

The values of the dielectric constant at lower applied electric fields ($E < 2Ec$) are mainly controlled by the domain contribution. Then, the decrease in the maximum dielectric constant as the film thickness decreases could be associated with the smaller volumetric contribution of the ferroelectric domains, relatively high number of pinning centers and non-switching interface layers. Nevertheless, other factors such as: the grain size, the film orientation, etc., should be taken into account because they change as the thickness decreases and affect directly or indirectly the ferroelectric domain contribution and the intrinsic contribution to the measured capacitance.

The values of the dielectric constant at high applied electric field, which is predominantly determined by the linear capacitance component (intrinsic contribution), increase as film thickness increase. This effect is a consequence of microstructural changes experimented by the PZT films as the thickness increases (i.e., changes in the film orientation, grain size and mechanical constraints imposed by the substrate). It is believed that among those, the substrate clamp-

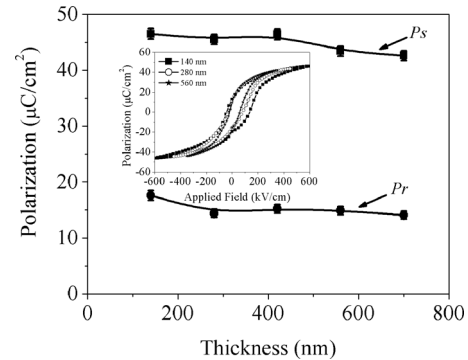


FIG. 8. Thickness dependences of remanent and saturated polarizations of PZT films.

ing is the main factor responsible for the increase in the intrinsic contribution to the dielectric constant.

2. Thickness dependence of the hysteresis loops in PZT films

Figure 8 shows the thickness dependences for the remanent (P_r) and saturated (P_s) polarizations. Both values, P_r and P_s , remain practically constant for all the samples, except for 140 nm thick PZT films, where remanent and saturated polarizations show a slight increase. Again, as in the C - V results, the thickness behavior of the polarization could be the consequence of several factors including film orientation,²⁴ grain size distribution,^{22,37} substrate clamping,¹⁶ and the peculiarities of domain wall motion (which is in fact sensitive to the above structural parameters).³⁸ It should be noted that the slightly higher values of P_s and P_r observed in the thinnest film (140 nm) could be achieved due to the above mentioned factors; however, it can be also a result of the higher electric field applied, necessary to reach the saturation.

The thickness dependence of the coercive field is shown in Fig. 9. This effect of thickness on the coercive field indicates that the domain reversal in PZT films becomes more difficult as the thickness decreases. Since reorientation of non- 180° domains is very limited in our films (due to the small grain sizes),¹⁶ domain reversal is mainly achieved by 180° domain wall motion.²³ With decreasing thickness, the domain wall motion becomes more difficult, and thus larger electric fields are needed to accomplish it.^{16,33} The rapid increase in the coercive field at thicknesses below 280 nm

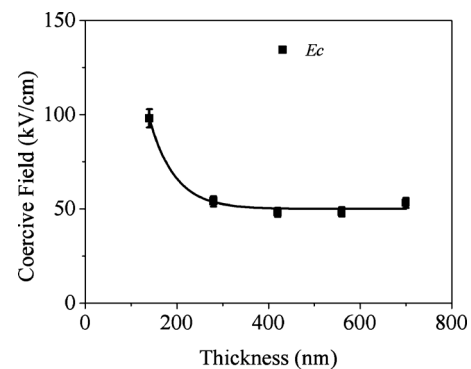


FIG. 9. Thickness dependence of the coercive field of PZT films.

suggest a drastic decrease in the 180° domain wall mobility and reduced nucleation. However, the dielectric loss, which is mainly related to the domain wall motion, does not decrease, as shown in Fig. 5. This consolidates the idea that the increase in the coercive field with decreasing film thickness should be affected by a dead layer at the ferroelectric-electrode interface. This layer decreases the driving electric field “seen” by the ferroelectric films as their thickness decreases, affecting the polarization and coercive field values.

D. Macroscopic piezoelectric properties as a function of thickness

Figure 9 illustrates the piezoelectric properties of PZT films as a function of film thickness. The piezoelectric coefficient (d_{33}) increases as the film thickness increases. Once again, the piezoelectric coefficient is directly related to the motion of non- 180° domain walls. For this reason, it is evident that with any increase in film thickness, non- 180° domain wall motions contribute to an increase in the piezoelectric response. The domain wall motions, and therefore the piezoelectric response, are indirectly affected by different factors such as: interface dead layer,¹⁶ film orientation,³⁹ grain size,³⁷ and substrate clamping,⁴⁰ which, in fact, are truly responsible for the increase in the piezoelectric coefficient as the film thickness increases.

It is believed that with the film thickness decrease the interface dead layer has largest influence in the charge injection process.^{16,41} Any increase in the injected charge due to the film thickness decrease might create new interface pinning centers and/or domain wall pinning centers (strong pinning of the non- 180° domain walls),^{11,16} which could reduce the macroscopic piezoelectric response. Other factor not directly related with the domain wall motion but with some influence in the formation of 180° and non- 180° domain walls is the film orientation. It is believed that (111)-oriented PZT films show higher affinity to non- 180° domain wall formation.²⁴ Based on this assumption (see, Fig. 1), it is reasonable to expect that as the thickness decreases, the formation of non- 180° domain walls is more probable, increasing the piezoelectric response.

An important issue not taken into account during the orientation contribution analysis is the film grain size. It can be true that the (111) orientation favors the non- 180° domain wall formation; however, small grain size is a physical impediment for the formation of non- 180° domain walls.⁴² As the film thickness decreases the grain size becomes smaller (Fig. 4) inhibiting the formation of grains with a *multidomain* structure. Grains with a *monodomain* structure impose a constraint on the piezoelectric orientation contribution and explain satisfactorily the observed trends in the piezoelectric behavior.

Substrate clamping is another factor that, independent of the ferroelectric materials, should affect the microscopic piezoelectric response of the films as their thickness decrease. It is well known that the clamping of the film to a rigid substrate results in significant reduction in effective electrostriction coefficients (compared to electrostriction coefficients of the unconstrained material) with subsequent decrease in

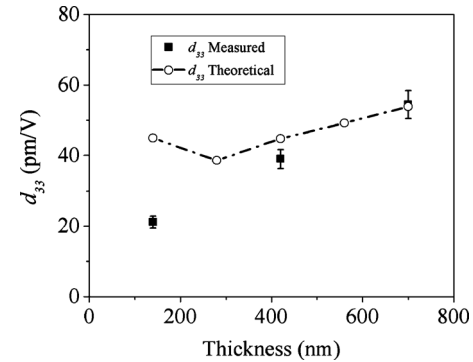


FIG. 10. Effective piezoelectric coefficients of PZT films measured by laser interferometry and those calculated using Eq. (4) (open circles) as a function of film thickness.

the d_{33} piezoelectric response.⁴³ This situation is intensified as the film thickness decreases due to the effect on the non- 180° domain wall motion, which could be partially or totally suppressed by the substrate clamping.⁴⁴

A theoretical analysis of the microscopic piezoelectric coefficient may be carried out based on the Eq. (4),⁴³

$$d_{33} = 2Q_{\text{eff}}(E)\epsilon_o\epsilon_{ff} \text{Pr}, \quad (4)$$

where Q_{eff} is the effective electrostriction coefficient (depending on the applied electric field). Theoretical d_{33} coefficient calculated based on a fixed effective electrostriction coefficient ($Q_{\text{eff}}=0.017 \text{ m}^4/\text{C}^2$) (Ref. 43) and the measured dielectric permittivity and remanent polarization, predicts some degradation of the piezoelectric properties as the film thickness decreases, except for the thinnest films where the calculated d_{33} coefficient increases, as shown in Fig. 10. A similar trend between the theoretical and measured values confirms the thickness effect on the piezoelectric properties of PZT thin films. The progressive discrepancy between theory and measurements as the film thickness decreases could be a consequence of an overestimation of the real value of Q_{eff} , which is not constant as assumed, being in fact dependent on substrate clamping, remanent polarization and film orientation.⁴³ This discrepancy could be also associated to the fact that the remanent polarization values used in Eq. (4) were obtained from P - V hysteresis loops, an instantaneous polarization value with no relaxation effects involved,^{6,43} however, d_{33} coefficients were measured after the attenuation of the relaxation process, due to the method adopted (see experimental procedure). On the other hand, it is well known that piezoelectric aging can be significant in thin films due to the influence of depolarizing fields, which are dependent on the clamping, domain configuration, etc.⁴⁵ These factors could lead to a significant underestimation of measured d_{33} coefficients.

Theoretic d_{33} value for the thinnest films (44.9 pm/V) is unrealistic and it was probably achieved due to a strong overestimation of the effective electrostriction coefficient used on the d_{33} calculation and the high value of the remanent polarization measured. As aforesaid, the Q_{eff} coefficient is a function of the substrate clamping, the remanent polarization and the film orientation. The increase in the substrate clamping and the remanent polarization and the changes in film orien-

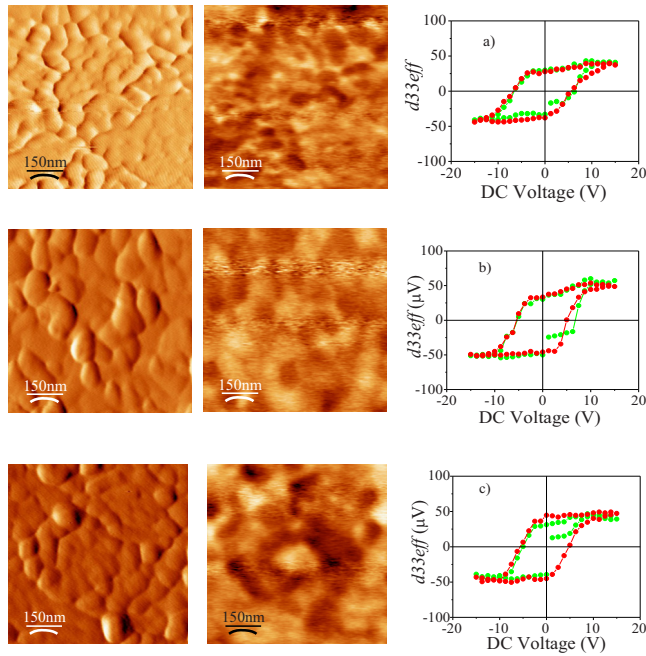


FIG. 11. (Color online) Topographic images, domain images, and piezoresponse of: (a) 140 nm, (b) 420 nm, and (c) 700 nm thick PZT films.

tation from (100) to (111) in the thinnest films (Fig. 1), decrease significantly the effective electrostriction coefficient and result in a strong decrease in the calculated d_{33} coefficients (e.g., a $Q_{\text{eff}}=0.01 \text{ m}^4/\text{C}^2$ results in a calculated d_{33} coefficient of 26.4 pm/V , close to the 21.2 pm/V for the measured d_{33} coefficient).

E. Microscopic piezoelectric properties as a function of the thickness

Macroscopic studies of ferroelectric films do not provide clear information about the exact nature of complex domain configurations and their evolution in the presence or absence of stress, applied external field, etc. Piezoresponse measurements, due to its nature,^{15,46} could help us to understand the effects of grain size, orientation, film-electrode interlayer, etc., on the dielectric and piezoelectric properties of PZT films as the film thickness decrease.

Figure 11 shows topography, domain distribution and piezoresponse curves of PZT films with three different thicknesses. The piezoresponse as a function of dc bias voltage obtained in black monodomain grains ($\sim 70 \text{ nm}$) shows that this property increases as the films thickness increase. The films show microscopic d_{33} values of $32.8 \text{ } \mu\text{V}$, $39.9 \text{ } \mu\text{V}$, and $44.6 \text{ } \mu\text{V}$ and coercive field (E_c) values of 6.3 V , 5.3 V , and 5.1 V (arbitrary units based on the signal measured by lock-in) in films with 140 nm, 420 nm, and 700 nm, respectively. These are not the true d_{33} values because in order to obtain the real values of the d_{33} coefficient it is necessary to calibrate the output signal from the photodiode with an x -cut quartz crystal⁴⁷ or to use the Harnegea and Alexe method,⁴⁸ which calibrate the output of the photodiode with the slope of the AFM force curve). However, these results show a

similar trend regarding the behavior of the d_{33} coefficient which is essential in the analysis and interpretation of the macroscopic properties.

If one considers that the effect of top film-electrode interlayer is avoided, only small grains sizes are analyzed and the electric field applied by the AFM tip is highly inhomogeneous and decays very fast across the thickness of the sample,⁴⁹ it is possible to expect that the piezoelectric response might be controlled by film orientation and substrate clamping. It is not easy to find a relationship between local grain orientation and macroscopic film orientation; and even more difficult to correlate the orientation with the piezoelectric properties. Nevertheless, one can suppose that the analyzed grains (as average) will probably have the same orientation as the film. Based on this supposition (see Fig. 1), it is expected that the local d_{33} coefficient increases as the film thickness decreases, contrary to the results shown in Fig. 11. As a consequence, it is possible to conclude that the most probable factor affecting the local piezoelectric response is the substrate clamping. The substrate clamping hypothesis is consistent with the piezoresponse values. The decrease in the local piezoelectric coefficient and the increase in the coercive field could be easily explained by the increase in the effect of substrate clamping as the film thickness decreases. On the other hand, Bdikin *et al.*, (Ref. 50) found that any variation in the intrinsic and extrinsic dielectric constants of the films would result in a different local piezoresponse, because it would generate different electric field distributions in the probed grains and their neighbors. This fact tells us that any changes in the surrounding grain size and polarization as the film thickness decreases could be factors that modified the local piezoelectric response.

The strong differences between the macroscopic and local piezoelectric trends as the film thickness decrease suggest that besides the abovementioned, other factors could be also responsible for the degradation observed in the macroscopic piezoelectric response. The lower effective applied electric field “seen” by the film and the higher number of injection charges (both due to the nonswitching interlayer) as the film thickness decreases could be the other factors responsible for these differences.

IV. CONCLUSIONS

Both the film orientation and the mean grain size change significantly in sol-gel derived PZT films as the film thickness increases. The effects of thickness on the microscopic dielectric, ferroelectric, and piezoelectric properties of the films were investigated and their behavior was explained based on film orientation, grain size, domain structure, domain wall motion, nonswitching interface layers, and substrate clamping. Serial capacitor and effective electrostrictive models were used to explain the influence of the nonswitching interface layer in the dielectric properties and the effect of substrate clamping in the microscopic piezoelectric response, respectively, as the film thickness decreases. The calculated values using these models are in correspondence with the measured values or they are, at least, interconnected. Finally, we can conclude that SFM is an important tool for

understanding both the macroscopic and microscopic properties because it explains the apparent contradiction between measurements performed at different sampling scales.

ACKNOWLEDGMENTS

J. Pérez acknowledges Portuguese Foundation for Science and Technology (FCT) for the financial support through his Post-Doctoral grant (Grant No. SFRH/BPD/16992/2004).

- ¹J. F. Scott and C. A. Paz de Araujo, *Science* **246**, 1400 (1989).
- ²F. Akasheh, T. Myers, J. D. Fraser, S. Bose, and A. Bandyopadhyay, *Sens. Actuators, A* **111**, 275 (2004).
- ³M. Kohli, C. Wuethrich, K. Brooks, B. Willing, M. Forster, P. Muralt, N. Setter, and P. Ryser, *Sens. Actuators, A* **60**, 147 (1997).
- ⁴D. E. Kotecki, J. D. Baniecki, H. Shen, R. B. Laibowitz, K. L. Saenger, J. J. Lian, T. M. Shaw, S. D. Athavale, C. Cabral, Jr., P. R. Duncombe, M. Gutsche, G. Kunkel, Y. J. Park, Y. Y. Wang, and R. Wise, *IBM J. Res. Dev.* **43**, 367 (1999).
- ⁵J. F. Scott, *Ferroelectric Memories* (Springer, Berlin, 2000).
- ⁶J. Pérez, P. M. Vilarinho, and A. L. Kholkin, *J. Mater. Res.* **20**, 1428 (2005).
- ⁷H. Rohrer, *Microelectron. Eng.* **32**, 5 (1996).
- ⁸H. Rohrer, *Microelectron. Eng.* **41–42**, 31 (1998).
- ⁹S. Li, J. A. Eastman, Z. Li, C. M. Foster, R. E. Newnham, and L. E. Cross, *Phys. Lett. A* **212**, 341 (1996).
- ¹⁰P. K. Larsen, G. J. M. Dormans, D. J. Taylor, and P. J. van Veldhoven, *J. Appl. Phys.* **76**, 2405 (1994).
- ¹¹J. F. M. Cillessen, M. W. J. Prins, and R. M. Wolf, *J. Appl. Phys.* **81**, 2777 (1997).
- ¹²V. Nagarajan, I. G. Jenkins, S. P. Alpay, H. Li, S. Aggarwal, L. Salamanca-Riba, A. L. Roytburd, and R. Ramesh, *J. Appl. Phys.* **86**, 595 (1999).
- ¹³M. Alexe and A. Gruverman, *Nanoscale Characterization of Ferroelectric Materials: Scanning Probe Microscopy Approach* (Springer-Verlag, Berlin, 2004).
- ¹⁴C. Durkan and M. E. Welland, *Ultramicroscopy* **82**, 141 (2000).
- ¹⁵A. Gruverman, O. Auciello, and H. Tokumoto, *Annu. Rev. Mater. Sci.* **28**, 101 (1998).
- ¹⁶J. Pérez, Ph.D. thesis, University of Aveiro, 2004.
- ¹⁷J. Pérez, P. M. Vilarinho, and A. L. Kholkin, *Thin Solid Films* **449**, 20 (2004); J. Pérez, P. M. Vilarinho, A. L. Kholkin, and A. Almeida, *Mater. Res. Bull.* **44**, 515 (2009).
- ¹⁸W. Y. Pan and L. E. Cross, *Rev. Sci. Instrum.* **60**, 2701 (1989).
- ¹⁹A. L. Kholkin, C. Wüthrich, D. V. Taylor, and N. Setter, *Rev. Sci. Instrum.* **67**, 1935 (1996).
- ²⁰www.nanosensors.com, "Scanning Probe Tips," Nanosensors Company (2003).
- ²¹www.nanotec.es, "Scanning Probe Microscopy Software," Nanotec Electrónica Company (2002).
- ²²J. K. Yang, W. S. Kim, and H. H. Park, *Appl. Surf. Sci.* **169–170**, 544 (2001).
- ²³F. Xu, S. Trolier-McKinstry, W. Ren, B. M. Xu, Z. L. Xie, and K. J. Hemker, *J. Appl. Phys.* **89**, 1336 (2001).
- ²⁴W. Gong, J. F. Li, X. Chu, Z. Gui, and L. Li, *J. Appl. Phys.* **96**, 590 (2004).
- ²⁵N. Kim, Ph.D. thesis, The Pennsylvania State University, 1994.
- ²⁶A. L. Roytburd, S. P. Alpay, V. Nagarajan, C. S. Ganpule, S. Aggarwal, E. D. Williams, and R. Ramesh, *Phys. Rev. Lett.* **85**, 190 (2000).
- ²⁷G. A. C. M. Spierings, G. J. M. Dormans, W. G. J. Moors, M. J. E. Ulenaers, and P. K. Larsen, *J. Appl. Phys.* **78**, 1926 (1995).
- ²⁸A. K. Tagantsev, I. Stolichnov, E. L. Colla, and N. Setter, *J. Appl. Phys.* **90**, 1387 (2001).
- ²⁹M. O. Eatough, D. Dimos, B. A. Tuttle, and W. L. Warren, *Mater. Res. Soc. Symp. Proc.* **361**, 111 (1995).
- ³⁰G. Arlt and N. A. Pertsev, *J. Appl. Phys.* **70**, 2283 (1991).
- ³¹S. K. Streiffner, C. Basceri, C. B. Parker, S. E. Lash, and A. I. Kingon, *J. Appl. Phys.* **86**, 4565 (1999).
- ³²Y. G. Wang, W. L. Zhong, and P. L. Zhang, *Phys. Rev. B* **51**, 5311 (1995).
- ³³C. Zhou, and D. M. Newns, *J. Appl. Phys.* **82**, 3081 (1997).
- ³⁴S. L. Miller, R. D. Nasby, J. R. Schwank, M. S. Rogers, and P. V. Dressendorfer, *J. Appl. Phys.* **68**, 6463 (1990).
- ³⁵A. K. Tagantsev, M. Landivar, E. Colla, and N. Setter, *J. Appl. Phys.* **78**, 2623 (1995).
- ³⁶A. K. Tagantsev and I. A. Stolichnov, *Appl. Phys. Lett.* **74**, 1326 (1999).
- ³⁷C. A. Randall, N. Kim, J. P. Kucera, W. Cao, and T. R. Shrout, *J. Am. Ceram. Soc.* **81**, 677 (1998).
- ³⁸N. Pertsev, A. Zembilgotov, and A. Tagantsev, *Phys. Rev. Lett.* **80**, 1988 (1998).
- ³⁹J. G. E. Gardeniers, Z. M. Rittersma, and G. J. Burger, *J. Appl. Phys.* **83**, 7844 (1998).
- ⁴⁰K. Lefki and G. J. M. Dormans, *J. Appl. Phys.* **76**, 1764 (1994).
- ⁴¹K. A. Vorotilov, M. I. Yanovskaya, and O. A. Dorokhova, *Integr. Ferroelectr.* **3**, 33 (1993).
- ⁴²K. Tanaka, K. Suzuki, D. Fu, K. Nishizawa, T. Miki, and K. Kato, *Jpn. J. Appl. Phys., Part 1* **43**, 6525 (2004).
- ⁴³A. L. Kholkin, E. K. Akdogan, A. Safari, P.-F. Chauvy, and N. Setter, *J. Appl. Phys.* **89**, 8066 (2001).
- ⁴⁴Q. M. Zhang, W. Y. Pan, S. J. Jang, and L. E. Cross, *J. Appl. Phys.* **64**, 6445 (1988).
- ⁴⁵A. L. Kholkin, A. K. Tagantsev, E. L. Colla, D. V. Taylor, and N. Setter, *Integr. Ferroelectr.* **15**, 317 (1997).
- ⁴⁶S. Jesse, A. P. Baddorf, and S. V. Kalinin, *Nanotechnology* **17**, 1615 (2006).
- ⁴⁷P. Muralt, *J. Micromech. Microeng.* **10**, 136 (2000).
- ⁴⁸C. Harnegea, A. Pignolet, M. Alexe, H. N. Lee, and D. Hesse, "Ferroelectric Polarization Switching as seen from Piezoresponse-AFM Measurements," Symposium D: Polarization Dynamics in Ferroic Materials (Fall 2001 Program) November 27–29 (2001).
- ⁴⁹D. E. Steinhauer, C. P. Vlahacos, F. C. Wellstood, S. M. Anlage, C. Canedy, R. Ramesh, A. Stanishevsky, and J. Melngailis, *Rev. Sci. Instrum.* **71**, 2751 (2000).
- ⁵⁰I. K. Bdikin, V. V. Shvartsman, S. H. Kim, J. M. Herrero, and A. L. Kholkin, *Mater. Res. Soc. Symp. Proc.*, **784**, C11.3 (2004).